

Electrostatic binding of ions by a self-assembled monolayer of N-(6-mercapto)hexylpyridinium on the Ag electrode as probed by surface enhanced Raman spectroscopy

Ieva Matulaitienė,

Laura Abariūtė,

Zenonas Kuodis,

Olegas Eicher-Lorka,

Algirdas Matijoška,

Gediminas Niaura*

Department of Organic Chemistry,
Center for Physical Sciences
and Technology,
Goštauto 9,
LT-01108 Vilnius,
Lithuania

The structure of a self-assembled monolayer formed from N-(6-mercapto)hexylpyridinium (MHP) on the Ag electrode and electrostatic binding of ions from a solution phase by the monolayer were studied in situ by surface enhanced Raman spectroscopy (SERS). The low frequency Ag–S stretching mode was detected at 236 cm^{-1} in agreement with the calculated value (230 cm^{-1}) for the $\text{Ag}_3\text{-MHP}$ complex. The $-\text{CH}_2-\text{CH}_2-\text{S}-\text{Ag}$ moiety was found to be in predominant *trans* conformation as was evident from the higher intensity of the C–S stretching band near 692 cm^{-1} comparing with the *gauche* conformer band at 626 cm^{-1} . Electrostatic attraction of NH_2SO_3^- , SO_4^{2-} , NO_3^- , BF_4^- , ClO_4^- , and PF_6^- anions by the MHP self-assembled monolayer on the Ag electrode was demonstrated by SERS. It was found that frequency of the totally symmetric stretching mode of surface bound anions shifts to lower wavenumbers comparing with ions in the solution phase. The higher shift corresponds to negatively larger Gibbs hydration energy of the anion.

Key words: self-assembled monolayers, SERS, pyridinium, sulfate, perchlorate, DFT

INTRODUCTION

The spontaneous self-assembled monolayers (SAMs) provide the possibility of changing metal surface properties in a controllable manner and have been found to be particularly valuable in numerous applications including fundamental studies of electron transfer phenomena [1, 2], construction of sensors and electrocatalytical systems [3], biotechnology, and photoelectronic industry [2]. Monolayers based on bifunctional thiol molecules containing a positively charged terminal group have been used for sensing of anions and

electrostatic attraction of biomolecules at the interface [3–12]. Contrary to the covalently wired peptides and proteins, electrostatically attracted biomolecules more readily preserve their native structure and function at the interface because of unrestricted mobility [5, 7, 13]. Monolayers with a terminal pyridinium functional group offer the positive charge at the interface in a wide solution pH range. The ability to attract counterions by SAMs depends on the structure and stability of surface attached organic molecules as well as on the nature of ions in the solution phase. Thus, for construction of surfaces with particular and predictable properties, detailed molecular level knowledge on the structure and function of monolayers is required.

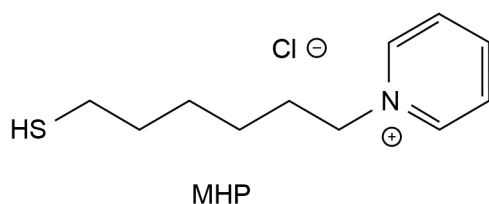
* Corresponding author. E-mail: gniaura@ktl.mii.lt

Surface-enhanced Raman spectroscopy (SERS) is one of the most sensitive vibrational spectroscopic tools for probing adsorbed molecules at roughened metals (mostly Au, Ag, and Cu) with molecular specificity and submonolayer sensitivity [14–16]. Previous SERS studies of molecules containing a pyridinium group revealed importance of ion pairing at the interface [4, 17–20]. It was demonstrated that N-methylpyridinium adsorbs at the silver electrode interface only in the presence of iodide ions [17]. Analysis of relative intensities of pyridinium SERS bands coupled with quantum chemical calculations and surface-selection rules revealed orientation of the ring with respect to the electrode surface [18, 19].

The present work aims at in situ SERS study of electrostatic binding of inorganic ions from the solution phase by the self-assembled monolayer formed from positively charged N-(6-mercapto)hexylpyridinium molecules on the Ag substrate.

EXPERIMENTAL

Millipore-purified water (18 M Ω cm) was used for preparation of solutions. N-(6-mercapto)hexylpyridinium (MHP) chloride (Scheme) was synthesized in our laboratory. The synthesis details will be published elsewhere. The most inorganic salts were ACS reagent grade and were purchased from Sigma-Aldrich Chemie GmbH (Germany). Sulfamic acid and sodium tetrafluoroborate were of “chemically pure” category, and they were acquired from RIAP (Kiev, Ukraine) and Reachim (Moscow, Russia), respectively. Sodium hexafluorophosphate was from Strem Chemicals, Inc. (Newburyport, MA).



Scheme. Structure of N-(6-mercapto)hexylpyridinium (MHP) chloride

Raman measurements were conducted with an Echelle type spectrometer RamanFlex 400 (PerkinElmer, Inc.) equipped with a thermoelectrically cooled (–50 °C) CCD camera and a fiber optic cable for excitation and collection of the Raman spectra [17]. The near-infrared diode laser provided an excitation beam at 785 nm. The excitation-scattering geometry was 180°. The laser power at the sample was restricted to 30 mW and the beam was focused to a 200 μ m diameter spot on the metal surface. The integration time was 300 s. Measurements were performed in a cylindrical glass cell with a quartz window. In order to reduce photo- and thermo-effects on the sample, the cell holder together with the working electrode was moved periodically with respect to the laser beam at a rate of about 15–25 mm/s with the help

of custom build equipment [21]. The wavenumber axis was calibrated by the polystyrene standard ASTM E1840, yielding ± 1 cm $^{-1}$ accuracy for narrow bands. Raman intensities were corrected by the NIST intensity standard SRM 2241. Parameters of overlapped bands were determined by fitting the experimental contour with Lorentzian-Gaussian form components by using the Grams/AI 8.0 software (Thermo Scientific Corp.).

The Ag electrode made by pressing the silver rod into Teflon was pretreated for SERS experiments in the following way. The electrode was first polished with soft sandpaper (P2500) and a 0.3 μ m alumina slurry (Buehler, USA) for refreshing the surface and sonicated in water-ethanol mixture (1 : 1, v/v) for 10 min. Then the electrode was roughened in 0.1 M KCl solution using four oxidation-reduction cycles in the potential range between –0.40 and 0.40 V vs. Ag/AgCl/KCl-saturated (scan rate 1 200 mV/s) with a pause for 30 s at the negative and 30 s at the positive potentials [22]. SAMs were formed by incubation of SERS active substrate in acetonitrile solution containing 10 $^{-3}$ M MHP for 16–24 h. After that the electrode was rinsed in acetonitrile, dried and transferred to the spectrometer stage holder for SERS measurements. SERS measurements were conducted in situ in aqueous solutions at the open circuit potential.

All calculations were performed using Gaussian for Windows package version G03W D.01 [23]. Geometry optimization and frequency calculations were accomplished with the density functional theory (DFT) method, using the B3LYP functional and 6–31++g(d,p) basis set for C, H, N, and S atoms, and LANL2DZ with ECP for Ag atoms. Calculated frequencies were scaled by the relation: $\nu' = \alpha(\nu) \cdot \nu$, where ν' and $\alpha(\nu)$ is the scaled frequency and scaling factor, respectively. The scaling factor was defined by the following equation [24]:

$$\alpha(\nu) = 1 - (1 - \alpha^F) \frac{\nu - \nu^0}{\nu^F - \nu^0} \quad (1)$$

using the parameters: $\alpha^F = 0.97$, $\nu^F = 4\,000$, and $\nu^0 = 600$. Calculated Raman scattering activities (S_j) were scaled by converting them to the Raman cross sections ($M\sigma/\Omega$) which are proportional to the Raman intensities and can be compared with the experimental data. The Raman scattering cross sections were calculated by using the following equation [25, 26]:

$$\frac{\partial \sigma_j}{\partial \Omega} = \left(\frac{2^4 \pi^4}{45} \right) \left(\frac{(\nu_0 - \nu_j)^4}{1 - \exp\left[\frac{-h\nu_j}{kT}\right]} \right) \left(\frac{h}{8\pi^2 c \nu_j} \right), \quad (2)$$

where ν_0 is the laser excitation frequency, ν_j is the vibrational frequency of the j th normal mode, and c and k are the universal constants. Predicted vibrational spectra were generated by using the Lorentzian function for broadening of Raman lines with 4 cm $^{-1}$ full width at half-maximum (FWHM) values.

RESULTS AND DISCUSSION

The main molecular groups of MHP, i. e. thiol, polymethylene chain, and charged pyridinium group (Scheme), can be characterized by Raman spectroscopy. Figure 1 compares the 0.5 M solution Raman spectrum of MHP with the SERS spectrum obtained after self-assembly of MHP (16 h) on the Ag electrode at the open circuit potential in the 0.01 M NaF solution. Table 1 summarizes the assignments of the MHP bands based on previous studies [4, 17–20, 27, 28] and our calculations. The disappearance of the well-defined feature at 2582 cm^{-1} due to S–H stretching vibration in the surface spectrum compared with solution one indicates cleavage of the corresponding bond upon adsorption. Formation of a covalent bond between the metal and adsorbate is evident from the appearance of intense low frequency feature at 236 cm^{-1} corresponding to Ag–S stretching vibration. A similar mode was observed recently at 235 cm^{-1} in analysis of formation of the imidazole ring self-assembled monolayer

formed from lipic acid histamide on the silver electrode [29]. Other vibrational modes involving motion of S atom are affected by bonding of MHP with silver as well. The first principles of quantum chemical calculations by modeling the adsorbed MHP with Ag_3 -MHP complex (Fig. 2) predict very well the frequencies of $\nu(\text{Ag-S})$ and $\nu(\text{C-S})_T$ vibrational modes (Table 1). The frequency of C–S stretching vibration is sensitive to *gauche* / *trans* isomerization of the $-\text{CH}_2-\text{CH}_2-\text{S}-\text{H}(\text{Ag})$ moiety [27, 28]. SERS spectrum evidences that upon MHP adsorption on the Ag surface the dominant conformation form is *trans* (692 cm^{-1}), while the *gauche* conformers are also visible at 626 cm^{-1} . The intensity ratio $I_{(\text{C-S})T}/I_{(\text{C-S})G}$ was found to be 2.3 indicating prevalence of the *trans* conformer at the interface. Interaction with the Ag surface induces shift of C–S vibrational modes to lower wavenumbers because of adsorption induced withdrawal of electron density from the C–S bond and the metal mass effect [27, 28]. Quantum chemical calculations predict very well the downshift of the $\nu(\text{C-S})_T$ mode upon formation of the Ag_3 -MHP complex

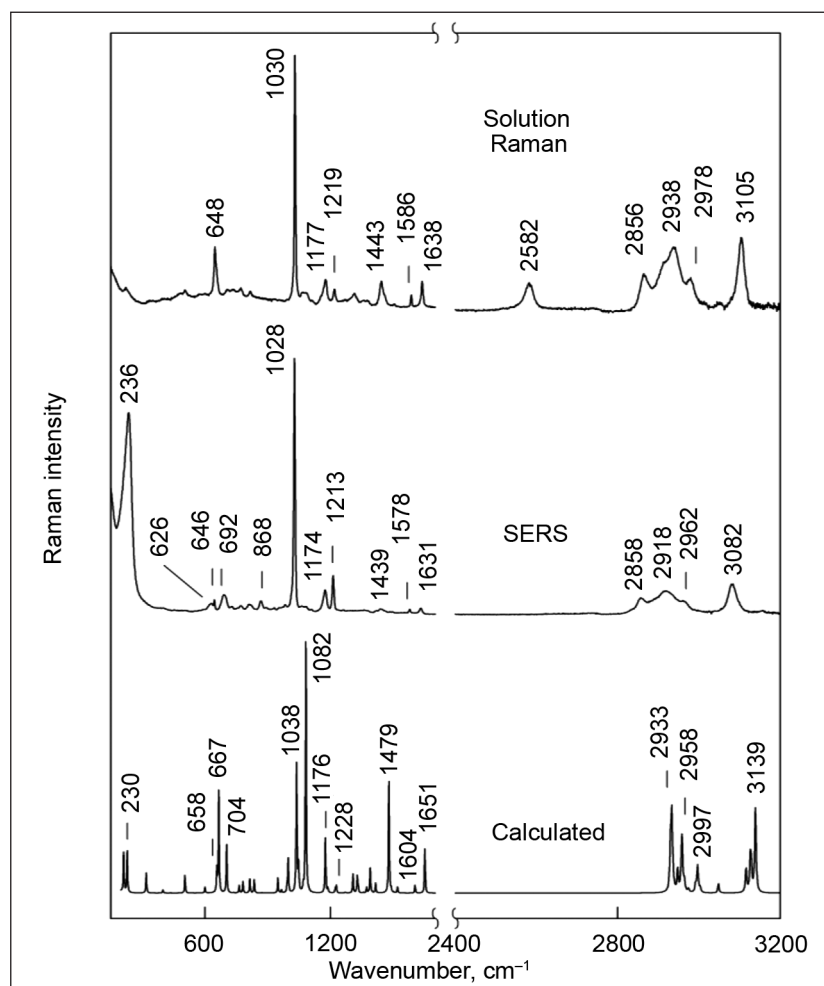


Fig. 1. Comparison of the aqueous solution (0.5 M) Raman spectrum of MHP, the SERS spectrum of MHP adsorbed at the Ag electrode in 0.01 M NaF solution, and the calculated spectrum of Ag_3 -MHP complex performed at DFT-B3LYP/6-31++g(d, p) basis set for C, H, N, and S atoms, and LANL2DZ with ECP for Ag atoms. Experimental spectra were normalized according to pyridinium ring ν_{12} mode near 1030 cm^{-1} . Water spectrum was subtracted from the solution spectrum of MHP. Excitation wavelength is 785 nm (30 mW)

Table 1. Assignments of MHP vibrational modes and peak positions of bands in solution (0.5 M) Raman spectrum, SERS spectrum from Ag electrode, and calculated values of Ag₃-MHP complex

Raman	Peak position, cm ⁻¹		Assignments ^a
	SERS	Calculated ^b	
3 105 s	3 082 s	3 139	v(=C–H) ring in-phase [$\nu_2(A_1)$] ^c
2 978 m	2 962 m	2 997	$\nu_3(C_7H_2)$ chain
2 938 s	2 918 s	–	$\nu_3(CH_2)_{FR}$ chain
2 856 m	2 858 m	2 933	$\nu_5(CH_2)$ chain
2 582 m	–	–	v(S–H)
1 638 m	1 631 w	1 651	v(C2=C3) + v(C6=C5) ring [$\nu_{8a}(A_1)$]
1 586 w	1 578 w	1 604	$\nu_{8s}(C3C4C5)$ + $\nu_{8s}(C2N1C6)$ ring [$\nu_{8b}(B_2)$]
1 443 m	1 440 m	1 479	$\delta(CH_2)$ scissoring, chain
1 219 w	1 213 s	1 228	$\beta(CH)$ ring [$\nu_{9a}(A_1)$]
1 177 m	1 174 m	1 176	v(C7–N1) + $\beta(CH)$ ring [$\nu_{15}(B_2)$]
1 030 vs	1 028 vs	1 038	$\nu_3(CCN)$ trigonal ring breathing [$\nu_{12}(A_1)$]
772 w	773 w	782	$\gamma(CH)$ ring [$\nu_{10b}(B_1)$]
732 w	692 m	704	v(C–S) _T
656 sh	626 m	–	v(C–S) _G
648 m	646 m	658	$\delta(CCN)$ in-plane, ring [$\nu_{6b}(B_2)$]
–	236 vs	230	v(Ag–S)

^aBased on references [4, 17–20, 27, 28] and calculations; ^bcalculated at B3LYP/6-31++g(d, p) basis set for C, H, N, and S atoms, and LANL2DZ with ECP for Ag atoms with hydrocarbon chain in *trans* conformation; ^cWilson vibration number of the benzene ring and vibration symmetry. Abbreviations: ν – stretching; δ – deformation; β – in-plane bending; γ – out-of-plane bending; G – *gauche*; T – *trans*

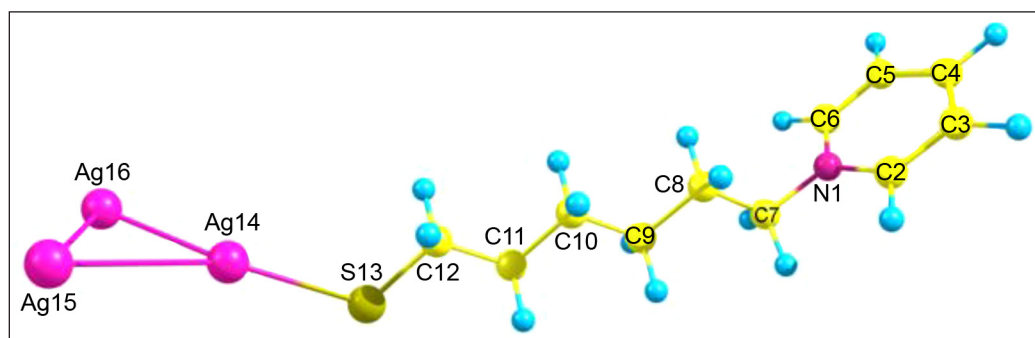


Fig. 2. Structure of the MHP complex with three silver atoms optimized at DFT-B3LYP/6-31++g(d, p) basis set for C, H, N, and S atoms, and LANL2DZ with ECP for Ag atoms

(Table 1). It should be noted that in the calculated spectrum the most intense band corresponds to C–C stretching vibration of the hydrocarbon chain in all-*trans* configuration at 1 082 cm⁻¹ (Fig. 1). However, the corresponding band was weak in the experimental SERS spectrum. It was found that the trigonal ring breathing mode at 1 028 cm⁻¹ (ν_{12}) dominates in both SERS and solution Raman spectra of MHP. Importantly, several pyridinium ring vibrational modes experience clear shift to lower wavenumbers upon adsorption of MHP on Ag. First of all, it concerns the high frequency v(=C–H) vibrational mode near 3 082 cm⁻¹ (Fig. 1). In addition, the downshift is obvious for well-defined ν_{8a} , ν_{8b} , ν_{9a} , and ν_{15} modes located in the SERS spectrum at 1 631, 1 578, 1 213, and 1 174 cm⁻¹, respectively. The downshift of frequencies might be associated with changes in water structure near the pyridinium ring and increased interaction between the neighboring MHP molecules in the adsorbed state. The position of two bands located at 1 028 (ν_{12}) and 646 cm⁻¹ (ν_{6b}) is close in both solution and SERS spectra.

The important function of the MHP monolayer is the ability to attract ions from the solution phase. Figure 3 compares SERS spectra of MHP adsorbed on the Ag electrode acquired in the aqueous solution containing 0.01 M of SO₄²⁻ and ClO₄⁻ anions. The difference spectrum clearly shows the intense positive-going peak at 933 cm⁻¹ and the low intensity negative-going band at 978 cm⁻¹ associated with totally symmetric vibrations of ClO₄⁻ and SO₄²⁻ anions, respectively [3, 30]. In the following series of experiments the reference SERS spectrum was acquired in the 0.01 M NaF solution. Such solution was chosen because the F⁻ ions are highly solvated and thus lower interaction strength with the monolayer is expected [3, 31]. At these conditions one might expect that complete exchange of anions at the interface will take place after immersion of the Ag/MHP monolayer in the solution containing the anions under investigation.

Figure 4 shows the dependence of difference SERS spectra on the nature of solution anion. Positive-going peaks

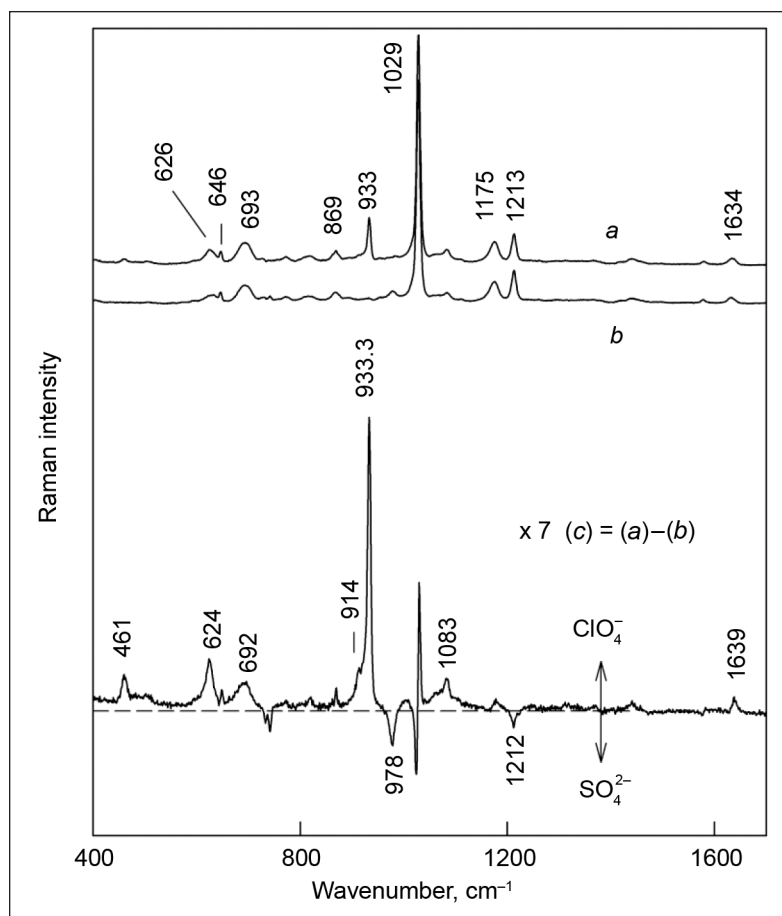


Fig. 3. SERS spectra of the MHP monolayer on the Ag electrode in (a) 0.01 M Na_2SO_4 and (b) 0.01 M NaClO_4 aqueous solutions. Difference spectrum (c) is also shown. Excitation wavelength is 785 nm (30 mW)

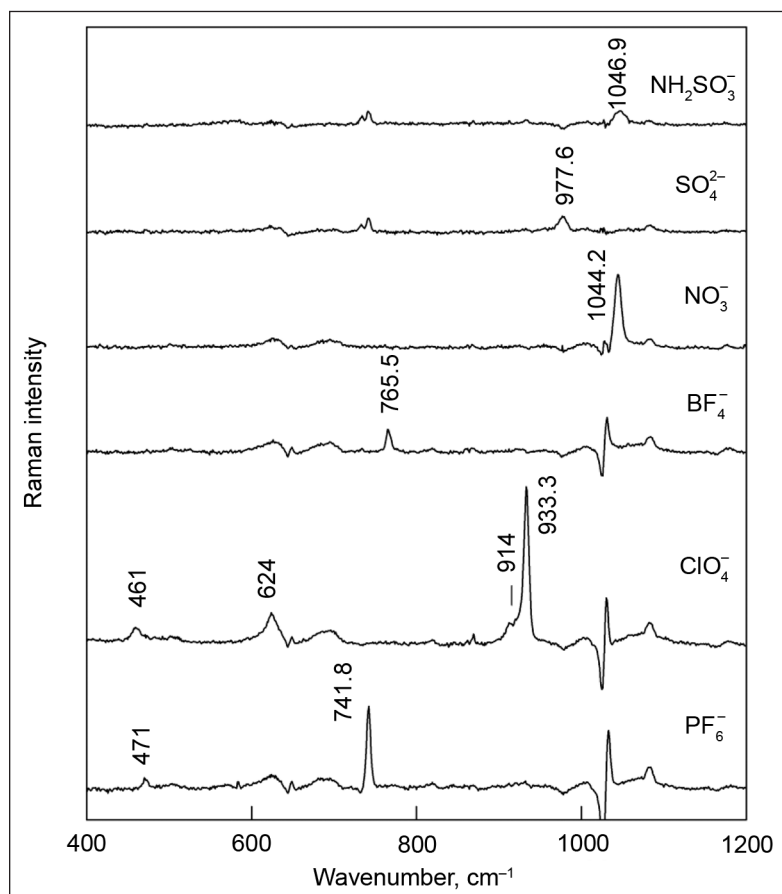


Fig. 4. Dependence of the difference SERS spectra of the MHP monolayer on the Ag electrode on the nature of the solution anion. The difference spectra were constructed by subtraction of the spectrum obtained in 0.01 M NaF solution from that recorded in 0.01 M Na_mX , where $\text{X}^{m-} = \text{NH}_2\text{SO}_3^-$, SO_4^{2-} , NO_3^- , BF_4^- , ClO_4^- , or PF_6^- . The difference spectra were normalized to the intensity of ν_{12} mode near 1030 cm^{-1} . Excitation wavelength is 785 nm (30 mW)

Table 2. Gibbs hydration energies (kJ mol⁻¹) and peak positions (cm⁻¹) of symmetric stretching vibration of anions in solution Raman and SERS spectra, and corresponding frequency-difference Δ (cm⁻¹) values

Anion	Gibbs hydration energy ^a	Peak position		$\Delta = \nu_{\text{Raman}} - \nu_{\text{SERS}}$
		Raman	SERS	
NH ₂ SO ₃ ⁻	–	1052.6	1046.9	5.7
SO ₄ ²⁻	-1080	982.0	977.6	4.4
NO ₃ ⁻	-300	1048.3	1044.2	4.1
BF ₄ ⁻	–	769.0	765.5	3.5
ClO ₄ ⁻	-205	934.9	933.3	1.6
PF ₆ ⁻	–	743.3	741.8	1.5

^aFrom reference [31].

correspond to totally symmetric stretching vibrations of studied anions electrostatically attracted by the MHP monolayer on Ag. Analysis of relative intensities of surface attracted SO₄²⁻ and ClO₄⁻ anions reveals that anions with lower negative Gibbs hydration energy (Table 2) are preferentially attracted by the MHP monolayer. The relative intensity of totally symmetric stretching vibrations for ClO₄⁻ and SO₄²⁻ anions in the solution Raman spectrum is similar, $I_{\text{R}}(\text{ClO}_4^-) / I_{\text{R}}(\text{SO}_4^{2-}) = 0.90$, while for surface bound anions the relative intensity in the SERS spectrum was found to be $I_{\text{SERS}}(\text{ClO}_4^-) / I_{\text{SERS}}(\text{SO}_4^{2-}) = 36$. Even if one assumes that surface concentration for SO₄²⁻ ions should be lower by a factor of two in order to compensate the positive MHP charge, the preferential binding of ClO₄⁻ anions with the monolayer is obvious. The peak positions of surface bound anions are slightly lower as compared with the solution phase data (Table 2). Importantly, the downshift is higher for anions exhibiting negatively larger Gibbs hydration energy. Such frequency shift might be associated with deformation of the solvation shell of the anions upon binding to the surface. The more pronounced deformation is expected for higher solvated anions.

CONCLUSIONS

We have used surface enhanced Raman spectroscopy to probe in situ the structure of the MHP monolayer on the Ag electrode and attraction of inorganic ions from the solution phase by the positively charged terminal pyridinium group of the monolayer. The density functional theory (DFT) calculations at the B3LYP/6-31++g(d, p) basis set for C, H, N, and S atoms, and LANL2DZ with ECP for Ag atoms have been used for interpretation of the observed SERS spectra. The surface bound MHP has been modeled by the Ag₃-MHP complex. Formation of the covalent Ag-S bond was demonstrated experimentally by appearance of the low-frequency $\nu(\text{Ag-S})$ vibrational mode at 236 cm⁻¹. The corresponding band in the calculated spectrum was predicted at 230 cm⁻¹. Two C-S stretching modes located at 692 and 626 cm⁻¹ have been assigned to *trans* and *gauche* conformers of adsorbed MHP, respectively. The intensity ratio $I_{(\text{C-S})\text{T}} / I_{(\text{C-S})\text{G}}$ was found to be 2.3 indicating prevalence of the *trans* conformer at the interface. Analysis of attraction of

anions by the monolayer has revealed that ClO₄⁻ anions which exhibit negatively lower Gibbs hydration energy adsorb preferentially at the interface compared with SO₄²⁻ anions. Binding with the surface has resulted in downshift of totally symmetric stretching frequency of the anions. It has been found that higher shift corresponds to negatively larger Gibbs hydration energy of the anion.

ACKNOWLEDGEMENTS

L. Abariūtė acknowledges Summer Undergraduate Research Fellowship Award from the Research Council of Lithuania.

Received 4 October 2013

Accepted 13 November 2013

References

1. J. F. Smalley, H. O. Finklea, C. E. D. Chidsey, et al., *J. Am. Chem. Soc.*, **125**, 2004 (2003).
2. A. Ulman, *Chem. Rev.*, **96**, 1533 (1996).
3. G. Valincius, G. Niaura, B. Kazakeviciene, Z. Talaikyte, M. Kazemkaite, E. Butkus, V. Razumas, *Langmuir*, **20**, 6631 (2004).
4. P. A. Mosier-Boss, S. H. Lieberman, *Langmuir*, **19**, 6826 (2003).
5. D. Zhou, X. Wang, L. Birch, T. Rayment, C. Abell, *Langmuir*, **19**, 10557 (2003).
6. L. L. Norman, A. Badia, *Langmuir*, **23**, 10198 (2007).
7. L. Sun, B. Johnson, T. Wade, R. M. Crooks, *J. Phys. Chem.*, **94**, 8869 (1990).
8. B. Gu, C. Ruan, W. Wang, *Appl. Spectrosc.*, **63**, 98 (2009).
9. P. A. Mosier-Boss, S. H. Lieberman, *Appl. Spectrosc.*, **55**, 1327 (2001).
10. P. A. Mosier-Boss, R. D. Boss, S. H. Lieberman, *Langmuir*, **16**, 5441 (2000).
11. C. Ruan, W. Wang, B. Gu, *Anal. Chim. Acta*, **567**, 114 (2006).
12. B. Kazakeviciene, G. Valincius, G. Niaura, Z. Talaikyte, M. Kazemkaite, V. Razumas, *J. Phys. Chem. B*, **107**, 6661 (2003).
13. B. Jin, G. X. Wang, D. Millo, P. Hildebrandt, X. H. Xia, *J. Phys. Chem. C*, **116**, 13038 (2012).
14. P. L. Stiles, J. A. Dieringer, N. C. Shah, R. P. Van Duyne, *Annu. Rev. Anal. Chem.*, **1**, 601 (2008).

15. K. Kneipp, H. Kneipp, I. Itzkan, R. R. Dasari, M. S. Feld, *J. Phys. Cond. Matter.*, **14**, R597 (2002).
16. G. Niaura, A. K. Gaigalas, V. L. Vilker, *J. Phys. Chem. B*, **101**, 9250 (1997).
17. V. Voiciuk, G. Valincius, R. Budvytyte, A. Matijoska, I. Matulaitiene, G. Niaura, *Spectrochim. Acta A*, **95**, 526 (2012).
18. K. A. Bunding, M. I. Bell, R. A. Durst, *Chem. Phys. Lett.*, **89**, 54 (1982).
19. E. Koglin, A. Tarazona, S. Kreisig, M. J. Schwuger, *Coll. Surf. A*, **123–124**, 523 (1997).
20. S. M. Kreisig, A. Tarazona, E. Koglin, M. J. Schwuger, *Langmuir*, **12**, 5279 (1996).
21. G. Niaura, A. K. Gaigalas, V. L. Vilker, *J. Raman Spectrosc.*, **28**, 1009 (1997).
22. E. Roth, G. A. Hope, D. P. Schweinsberg, W. Kiefer, P. M. Fredericks, *Appl. Spectrosc.*, **47**, 1794 (1993).
23. M. J. Frisch, G. W. Trucks, H. B. Schlegel, G. E. Scuseria, M. A. Robb, J. R. Cheeseman, J. A. Montgomery Jr., T. Vreven, K. N. Kudin, J. C. Burant, J. M. Millam, S. S. Iyengar, J. Tomasi, V. Barone, B. Mennucci, M. Cossi, G. Scalmani, N. Rega, G. A. Petersson, H. Nakatsuji, M. Hada, M. Ehara, K. Toyota, R. Fukuda, J. Hasegawa, M. Ishida, T. Nakajima, Y. Honda, O. Kitao, H. Nakai, M. Klene, X. Li, J. E. Know, H. P. Hratchian, J. B. Cross, C. Adamo, J. Jaramillo, R. Gomperts, R. E. Stratmann, O. Yazyev, A. J. Austin, R. Cammi, C. Pomelli, J. W. Ochterski, P. Y. Ayala, K. Morokuma, G. A. Voth, P. Salvador, J. J. Dannenburg, V. G. Zakrzewski, S. Dapprich, A. D. Daniels, M. C. Strain, O. Farkas, D. K. Malick, A. D. Rabuck, K. Raghavachari, J. B. Foresman, J. V. Ortiz, A. Liashenko, P. Piskorz, I. Komaromi, R. L. Martin, D. J. Fox, T. Keith, M. A. Al-Laham, C. Y. Peng, A. Nanayakkara, M. Challacombe, P. M. W. Gill, B. Johnson, W. Chen, M. W. Wong, C. Gonzalez, J. A. Pople, *Gaussian 03, Revision D.01*, Gaussian, Inc., Wallingford, CT (2004).
24. L. Riauba, G. Niaura, O. Eicher-Lorka, E. Butkus, *J. Phys. Chem. A*, **110**, 13394 (2006).
25. P. L. Polavarapu, *J. Phys. Chem.*, **94**, 8106 (1990).
26. G. A. Guirgis, P. Klaboe, S. Shen, et al., *J. Raman Spectrosc.*, **34**, 322 (2003).
27. M. A. Bryant, J. E. Pemberton, *J. Am. Chem. Soc.*, **113**, 3629 (1991).
28. M. A. Bryant, J. E. Pemberton, *J. Am. Chem. Soc.*, **113**, 8284 (1991).
29. I. Matulaitiene, Z. Kuodis, O. Eicher-Lorka, G. Niaura, *J. Electroanal. Chem.*, **700**, 77 (2013).
30. G. Niaura, A. Malinauskas, *J. Chem. Soc. Faraday Trans.*, **94**, 2205 (1998).
31. A. Yuchi, S. Kuroda, M. Takagi, Y. Watanabe, S. Nakao, *Anal. Chem.*, **82**, 8611 (2010).

Ieva Matulaitienė, Laura Abariūtė, Zenonas Kuodis,
Olegas Eicher-Lorka, Algirdas Matijoška, Gediminas Niaura

ELEKTROSTATINĖS JONŲ IR SAVITVARKIO MONOSLUOKSNIO, SUFORMUOTO IŠ N-(6-MER- KAPTO)HEKSILPIRIDINIO MOLEKULIŲ ANT Ag ELEKTRODO, SAŲVEIKOS TYRIMAS PAVIRŠIAUS SUSTIPRINTOS RAMANO SPEKTROSKOPIJOS METODU

Santrauka

Paviršiaus sustiprintos Ramano spektroskopijos (PSRS) metodu tirta savitvarkio monosluoksnio, suformuoto iš N-(6-merkapt) heksilpiridinio (MHP) molekulių ant Ag elektrodo, struktūra ir anijonų sąveika su monosluoksniu. Žemo dažnio juosta ties 236 cm^{-1} buvo priskirta Ag–S valentiniam virpesiui. Šį priskyrimą patvirtino modelinio komplekso $\text{Ag}_3\text{-MHP}$ kvantų chemijos skaičiavimai, kurie parodė, kad Ag–S virpesio dažnis turėtų būti ties 230 cm^{-1} . Analizuojant C–S juostas nustatyta, kad $-\text{CH}_2-\text{CH}_2-\text{S}-\text{Ag}$ molekulinės grupės vyraujanti konformacija yra *trans*. Atitinkamos juostos ties 692 cm^{-1} intensyvumas buvo didesnis, palyginti su *goš* konformero juostos ties 626 cm^{-1} intensyvumu. PSRS metodu parodyta, kad MHP monosluoksnis elektrostatiškai pritraukia NH_2SO_3^- , SO_4^{2-} , NO_3^- , BF_4^- , ClO_4^- ir PF_6^- anijonus. Nustatyta, kad adsorbuotų anijonų visiškai simetrinio virpesio dažnis sumažėja, palyginti su tirpale esančiais anijonais. Dažnio sumažėjimas yra tiek didesnis, kiek didesnė neigiama anijono Gibso hidracijos energija.